








Five New Heartbeat Star Systems with Tidally Excited Oscillations Discovered Based on TESS Data

MIN-YU LI ¹, SHENG-BANG QIAN ^{2,3,*}, AI-YING ZHOU,⁴ LI-YING ZHU ^{1,5}, WEN-PING LIAO ^{1,5}, ER-GANG ZHAO,¹
XIANG-DONG SHI ¹, FU-XING LI ^{2,3} AND QI-BIN SUN ^{2,3}

¹Yunnan Observatories, Chinese Academy of Sciences, Kunming 650216, People's Republic of China

²Department of Astronomy, School of Physics and Astronomy, Yunnan University, Kunming 650091, People's Republic of China

³Key Laboratory of Astroparticle Physics of Yunnan Province, Yunnan University, Kunming 650091, People's Republic of China

⁴National Astronomical Observatories, Chinese Academy of Sciences, A20 Datun Road, Chaoyang District, Beijing 100101, People's Republic of China

⁵University of Chinese Academy of Sciences, No.1 Yanqihu East Road, Huairou District, Beijing 101408, People's Republic of China

ABSTRACT

Heartbeat stars (HBSs) with tidally excited oscillations (TEOs) are ideal astrophysical laboratories for studying the internal properties of the systems. In this paper, five new HBSs exhibiting TEOs are discovered using TESS photometric data. The orbital parameters are derived using a corrected version of Kumar et al.'s model based on the Markov Chain Monte Carlo (MCMC) method. The TEOs in these objects are examined, and their pulsation phases and modes are identified. The pulsation phases of the TEOs in TIC 266809405, TIC 266894805, and TIC 412881444 are consistent with the dominant $l = 2$, $m = 0$, or ± 2 spherical harmonic. For TIC 11619404, although the TEO phase is close to the $m = +2$ mode, the $m = 0$ mode cannot be excluded because of the low inclination in this system. The TEO phase in TIC 447927324 shows a large deviation ($> 2\sigma$) from the adiabatic expectations, suggesting that it is expected to be a traveling wave rather than a standing wave. In addition, these TEOs occur at relatively low orbital harmonics, and we cautiously suggest that this may be an observational bias. These objects are valuable sources for studying the structure and evolution of eccentricity orbit binaries and extending the TESS HBS catalog with TEOs.

Keywords: Binary stars (154) – Elliptical orbits (457) – Stellar oscillations (1617) – Pulsating variable stars (1307)

1. INTRODUCTION

Heartbeat stars (HBSs) are a subclass of detached binaries with eccentric orbits. They are named for the shape of their light curve, which resembles an electrocardiogram (Thompson et al. 2012). Meanwhile, tidally excited oscillations (TEOs) are an essential property of HBSs that can be used to probe the internal structure of the star (Guo et al. 2020). They are induced by the phase-dependent tides in binary stars with eccentric orbits (Zahn 1975; Kumar et al. 1995; Fuller 2017; Jackiewicz 2021; Kołaczek-Szymański et al. 2022), and can occur in some of the HBSs. Theoretical work is extensive, but it is challenging to detect with ground-based telescopes due to the small amplitude and short duration variations in their light curves (Fuller 2017). Since the Kepler satellite (Borucki et al. 2010) provides long baselines and high-precision photometric data for such small variations, several Kepler HBSs and their TEOs have been studied in a series of papers (Welsh et al. 2011; Fuller & Lai 2012; Burkart et al. 2012; O'Leary & Burkart 2014; Hambleton et al. 2013, 2016; Guo et al. 2017, 2019, 2020; Guo 2020; Guo et al. 2022; Li et al. 2024a,b).

On the other hand, the Transiting Exoplanet Survey Satellite (TESS; Ricker et al. (2015)) also provides a valuable opportunity to study HBSs and their TEOs. Kołaczek-Szymański et al. (2021) studied 20 TESS HBSs, seven of which have TEOs. Wang et al. (2023) reported the linear and nonlinear TEOs and δ Sct pulsations in HBS FX UMa. The interesting HBS MACHO 80.7443.1718 (TIC 373840312) has also been studied in a number of papers (Jayasinghe et al. 2019, 2021; Kołaczek-Szymański & Różański 2023; MacLeod & Loeb 2023; Kołaczek-Szymański et al. 2024). However,

* E-mail: qiansb@ynu.edu.cn

given the high resolution and continuous release of TESS photometric data, the potential of studying HBSs and their TEOs based on TESS data has not yet been fully exploited.

Thanks to the continuous release of the TESS data, we have discovered five new TESS HBSs and their TEOs in this paper. Section 2 presents the analytic procedure for these objects, including the HBS modeling, the TEO detection approach, and the pulsation phases and mode identification of the TEOs. Section 3 presents the results of the analytic procedure. Section 4 discusses the results and concludes our work.

2. DATA AND ANALYSES

2.1. Data Reduction

The TESS was launched in 2018 as a space-based, all-sky optical exoplanet survey mission. The field of view is 24×96 degrees, and the observation sector is approximately 27 days for a given position in the sky. We use the light curve data processed by TESS-SPOC (the TESS Science Processing Operations Center) and the MIT QLP (the MIT Quick-Look Pipeline), downloaded by using the `lightkurve` package (Lightkurve Collaboration et al. 2018). We visually inspected the light curves of each object and selected data sources with low scatter and significant heartbeat signals for analysis. Columns 5 and 6 in Table 1 represent the selected data source and sector(s). We also removed obvious outliers by visual inspection and detrended the data using the Locally Weighted Scatter-plot Smoothing (LOWESS) approach (Cleveland 1979).

2.2. Modeling

We fit the corrected version of the Kumar et al. (1995) model (K95⁺ model) to the light curves. The K95⁺ model is shown in Eq. (1) and differs from Eq. (44) in Kumar et al. (1995) in that the sign before ω is changed from minus to plus (Wrona et al. 2022):

$$\frac{\delta F}{F}(t) = S \cdot \frac{1 - 3 \sin^2 i \sin^2(\varphi(t) + \omega)}{(R(t)/a)^3} + C, \quad (1)$$

The K95⁺ model approximates the equilibrium tidal deformation with a sum of all dominant modes, with $l = 2$ and $m = 0, \pm 2$ (Kołaczek-Szymański et al. 2021), and contains seven parameters: orbital period (P), eccentricity (e), orbital inclination (i), argument of periastron (ω), the epoch of periastron message (T_{0p}), the amplitude scaling factor (S), and the fractional flux offset (C) (Li et al. 2023).

We use the Markov Chain Monte Carlo (MCMC) method with the `emcee` v3.1.2 Python package (Foreman-Mackey et al. 2013) to fit the light curves, following the fitting approach in Li et al. (2023). The parameters and their uncertainties of the five HBSs are derived and presented in Table 2, where the first column is the TESS ID; columns 2–8 represent the seven parameters of the K95⁺ model.

2.3. Detection of TEOs

We then use the analytic procedure in Li et al. (2024b) to examine the harmonic TEOs in these HBSs. The Fourier spectra are derived using the FNPEAKS¹ code. The mean noise level of each frequency, N , is derived as the mean amplitude in the frequency range $\pm 1 \text{ d}^{-1}$. Only frequencies with a signal-to-noise ratio (S/N) greater than 4.0 are used for TEO analysis. If the frequency f satisfies at least one of the following equations, it is considered a harmonic TEO candidate:

$$|n - f/f_{\text{orb}}| < 0.01, \quad (2)$$

$$|n - f/f_{\text{orb}}| < 3\sigma_{f/f_{\text{orb}}}, \quad (3)$$

where n is the harmonic number, $f_{\text{orb}} = 1/P$ is the orbital frequency, $\sigma_{f/f_{\text{orb}}} = \sqrt{P^2\sigma_f^2 + f^2\sigma_P^2}$ is the uncertainty of f/f_{orb} according to Kołaczek-Szymański et al. (2021) and Wrona et al. (2022), σ_f and σ_P stand for the uncertainties of f and P , respectively. σ_f is estimated following Kallinger et al. (2008). P and σ_P are represented in Table 2. Following the analytic procedure (Li et al. 2024b), we derive the harmonic TEO for each HBS. Since there is only one harmonic TEO for each HBS, we combine them into Table 3 for presentation.

¹ <http://helas.astro.uni.wroc.pl/deliverables.php?active=fnpeaks>

2.4. Pulsation phases and mode identification

We then further identify the pulsation phases and mode of these TEOs following Li et al. (2024a). The pulsation phases of the TEOs for dominant modes of spherical harmonic degree $l = 2$ can be expressed by Equation (4) is based on the following assumptions: (1) the axes of the pulsation, spin, and orbit are all aligned; (2) the pulsations are adiabatic and the TEOs are standing waves; (3) the TEOs are not fine-tuned (O’Leary & Burkart 2014; Guo et al. 2020):

$$\phi_{l=2,m} = 0.25 + m\phi_0, \quad (4)$$

where azimuthal order $m = 0, \pm 2$, $\phi_0 = 0.25 - \omega/360^\circ$; ω is the argument of periastron. All phases can be measured with respect to the epoch of periastron passage T_{0p} and are in units of 360° . In addition, ω and T_{0p} are presented in Table 2. We also perform a standard prewhitening procedure using Period04 (Lenz & Breger 2005), which calculates the uncertainties according to Montgomery & O’Donoghue (1999), to derive the phases of the harmonic frequencies. Note that since the phase is measured relative to T_{0p} in the Fourier spectrum, the time of each data point in the photometric light curves should subtract T_{0p} before Fourier analysis. Following the analytic procedure in Li et al. (2024a), we identify the pulsation phases and mode of these TEOs and show them in each panel (d) of Figures 1 – 5.

3. RESULTS

Table 1 shows the basic parameters of the five TESS HBSs, where columns 5 and 6 indicate the data source and sectors used in this paper.

Table 1. Basic parameters of the five TESS HBSs.

TESS ID	Simbad main ID	Coords (J2000)	V(mag)	D.S.	sector(s)
11619404	HD 188060B	19 52 19.62 +25 51 43.59	8.45	(2)	41
266809405	HD 62629	07 45 08.94 +02 27 34.91	9.19	(1)	34
266894805	HD 62811	07 45 47.63 +02 33 35.46	7.97	(1)	34
412881444	BD+63 1793	21 58 43.06 +64 37 55.89	9.41	(1)	57,58
447927324	HD 77812	09 03 07.87 –45 22 24.43	9.03	(1)	62

NOTE—The first column is the TESS ID; columns 2–4 are the basic parameters of the objects. Column 5 shows the data source: (1) TESS-SPOC data; (2) MIT QLP data. Column 6 shows the sector(s) used for analysis.

Table 2 shows the parameters of the K95⁺ model derived in section 2.2.

Table 2. Parameters of the K95⁺ model fitted to the light curves of the five TESS HBSs.

TESS ID	P (d)	e	i ($^\circ$)	ω ($^\circ$)	T_{0p} (TJD)	S ($\times 10^{-4}$)	C ($\times 10^{-4}$)
11619404	5.41884(57)	0.3650(29)	11.99(38)	176.1(11)	2423.1719(19)	36.28(58)	-26.24(36)
266809405	9.9644(51)	0.4735(20)	46.11(23)	24.8(10)	2235.555(10)	4.439(50)	-0.573(62)
266894805	5.78914(57)	0.39915(81)	50.41(11)	66.11(22)	2234.0678(19)	8.319(43)	-0.771(41)
412881444	11.26990(71)	0.46013(77)	53.31(11)	134.54(25)	2856.9588(31)	7.300(36)	-0.203(48)
447927324	3.26596(40)	0.1865(14)	29.574(96)	154.24(41)	2989.7078(29)	29.44(21)	-17.05(18)

NOTE—The first column is the TESS ID; columns 2–8 are the seven parameters in the K95⁺ model. The unit of T_{0p} is TJD=BJD–2,457,000.

Table 3 shows the TEO parameters of these HBSs, where columns 2 – 4 are derived from section 2.3, and columns 5 – 8 are derived from section 2.4.

Table 3. TEO parameters of the five TESS HBSs.

TESS ID	n	Δn	$3\sigma - \Delta n $	Frequency (day^{-1})	Amplitude (mmag)	Phase	S/N
11619404	6	-0.001	0.035355	1.10758(75)	0.545(17)	0.808(5)	6.51
266809405	6	0.047	0.068229	0.6052(11)	0.316(12)	0.912(6)	4.81
266894805	9	0.009	0.034922	1.5556(10)	0.2316(85)	0.129(6)	6.73
412881444	12	0.004	0.028905	1.06476(33)	0.1968(62)	0.215(5)	6.63
447927324	3	0.010	0.016348	0.92148(57)	0.3564(90)	0.455(4)	5.1

NOTE—The first column is the TESS ID; n is the harmonic number of the TEO; $\Delta n = f/f_{\text{orb}} - n$, where f is the detected frequency (column 5); a positive value in column 4 indicates that it satisfies Eq. (3); column 6 is the amplitude; column 7 is the phase; S/N is the signal-to-noise ratio.

3.1. TIC 11619404 (Figure 1)

This is a 5.4 day HBS system, with an eccentricity of 0.365 and a low inclination of $11^\circ.99$. The TEOs are obvious in panel (b), and panel (c) shows that the harmonic number is $n = 6$. Since the ω of $176^\circ.1$ is very close to 180° , the $m = \pm 2$ strips are close to the gray strips, making it difficult to identify the modes. As shown in panel (d), the $n = 6$ harmonic is close to the $m = +2$ mode. However, Guo et al. (2020) have concluded that a low inclination (less than 30°) would favor the $m = 0$ mode. Given the low inclination in this system, we suggest that the $m = 0$ mode cannot be excluded either.

3.2. TIC 266809405 (Figure 2)

This is a period of 9.96 day HBS system with an eccentricity of 0.474, an intermediate inclination of $46^\circ.1$, and an argument of periastron ω of $24^\circ.8$. The $n = 6$ orbital harmonic stands out clearly in panel (c) of Figure 2. Panel (d) shows that the phase of the $n = 6$ harmonic is consistent with the $m = -2$ mode.

3.3. TIC 266894805 (Figure 3)

This is a 5.8 day HBS system, with an eccentricity of 0.399, an intermediate inclination of $50^\circ.41$, and an argument of periastron ω of $66^\circ.11$. The $n = 9$ orbital harmonic stands out clearly in panel (c) of Figure 3. Panel (d) shows that the phase of the $n = 9$ harmonic is consistent with the $m = -2$ mode.

3.4. TIC 412881444 (Figure 4)

This is a period of 11.3 day HBS system, with an eccentricity of 0.460, an inclination of $53^\circ.31$, and an argument of periastron ω of $134^\circ.54$, as shown in Figure 4. The $n = 12$ harmonic is clearly visible in panel (c). Panel (d) shows that its pulsation phase is close to the $m = 0$ mode.

3.5. TIC 447927324 (Figure 5)

This is a short-period of 3.3 day HBS system, with a low eccentricity of 0.187, a low inclination of $29^\circ.57$, and an argument of periastron ω of $154^\circ.24$, as shown in Figure 5. Panel (c) shows that the TEO candidate is the $n = 3$ harmonic. In addition, the $n = 4$ and 5 harmonics also exist, but given their lower S/N (≤ 4.0), we exclude them as the TEO candidates. However, the $n = 3$ harmonic shows a large deviation ($> 2\sigma$) from the adiabatic expectations in panel (d). Given the presence of obvious TEOs in panels (a) and (b), we suggest that the $n = 3$ harmonic is expected to be a traveling wave rather than a standing wave.

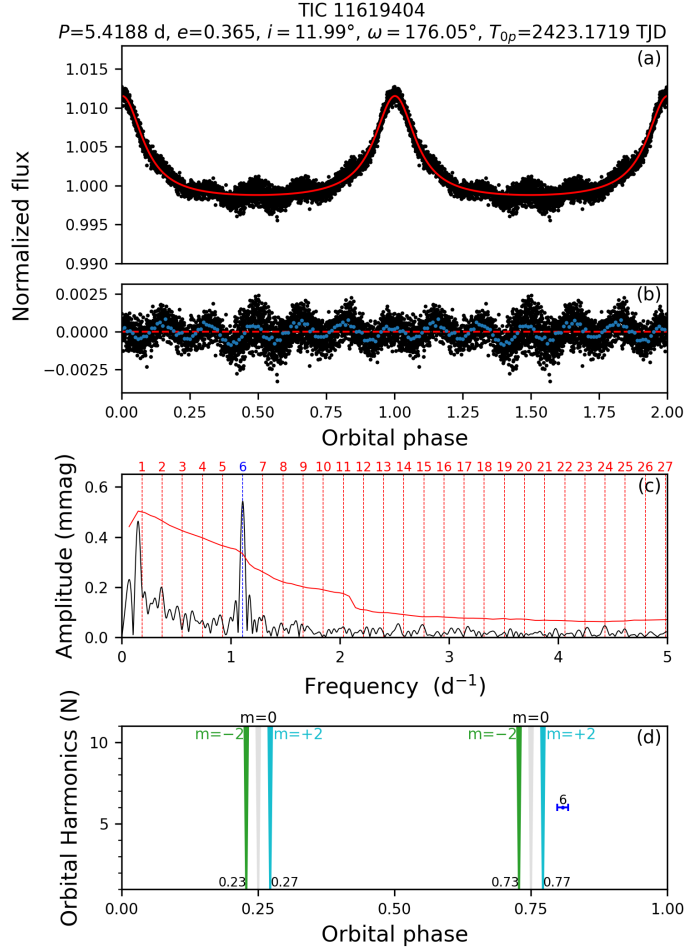


Figure 1. The analytic procedure for TIC 11619404. Panel (a): The K95⁺ model (solid red line) fitted to the phase-folded light curve (black dots). Panel (b): The residuals of the fit in panel (a), and the blue dots are medians in 0.01 phase bins. Panel (c): The Fourier spectrum of the residuals from panel (b). The red and blue vertical dashed lines represent the orbital harmonics n ; the blue lines indicate that they are harmonic TEOs. The solid red line shows the level of $S/N = 4.0$. Panel (d): The pulsation phases of the TEOs. The gray, light blue, and green strips indicate the $m = 0, +2$, and -2 modes, respectively. The phases of the $m = +2, -2$ modes are shown next to the strips. The width of the strips results from the uncertainties of T_{0p} and ω . The blue circle represents a TEO with its harmonic number n ; the size corresponds to its amplitude; the error bar corresponds to the uncertainty of its phase.

4. DISCUSSIONS AND CONCLUSIONS

The components in HBS systems are distorted by the time-varying tidal potential of the companion star, and the response of the components can usually be divided into two parts: the equilibrium tide and the dynamical tide. The equilibrium tide contributes to the “heartbeat” feature, while the dynamic tide is made up of TEOs that are visible in all phases of the orbit (Fuller 2017). To study TEOs, the contribution of the equilibrium tide must first be subtracted from the light curves. The remaining dynamical tide, which contains features of TEOs, can then be used to perform Fourier spectral analysis (Guo et al. 2020). Meanwhile, the K95⁺ model can be used to model these non-eclipsing HBSs (Li et al. 2023).

Note that the K95⁺ model does not take into account the irradiation/reflection effects or Doppler beaming (Kołaczek-Szymański et al. 2021). Therefore, the derived parameters may show some deviations. However, based on previous works, we believe that such deviations are limited. First, the orbital period P , the eccentricity e , and the argument of periastron ω derived from the K95⁺ model are usually reliable (Guo et al. 2020; Li et al. 2023). Second, the inclination i can indeed have deviations in different cases (Wrona et al. 2022; Li et al. 2023). In particular, it is possible for i to be overestimated if the obtained inclination is too high and there is no eclipse in the light curve. Third, ω derived

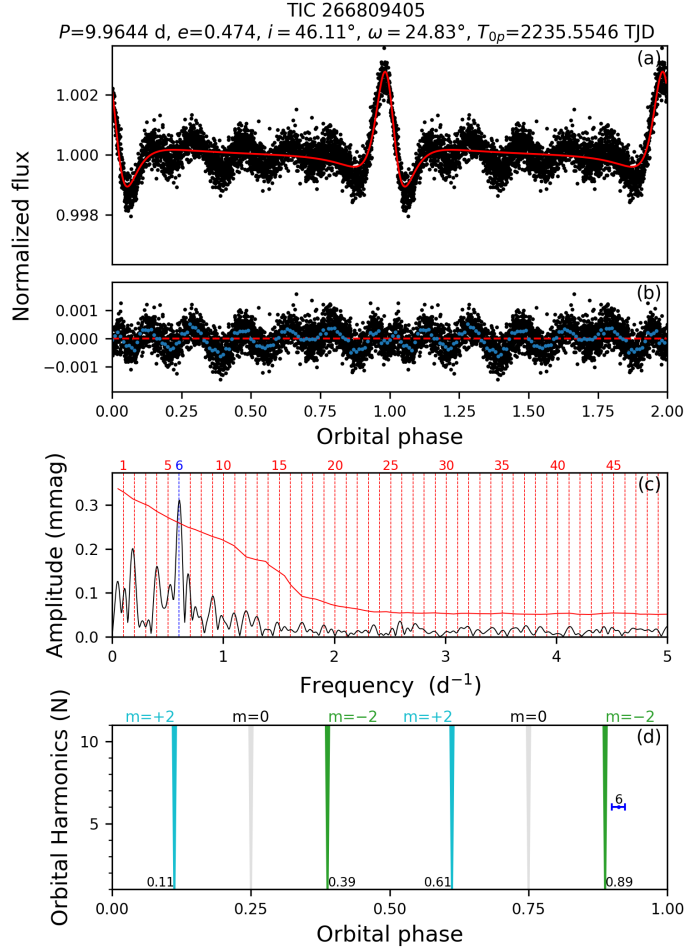


Figure 2. Same as Fig. 1 for TIC 266809405.

from the different approaches may have some slight differences. In this case, a comprehensive consideration of these different values is required. Therefore, these differences do not significantly affect the mode identification results (Li et al. 2024a). In summary, the results obtained from these approaches in this work are generally reliable.

In this work, we discover five new TESS HBSs that exhibit TEOs. First, we derive the orbital parameters using the K95⁺ model based on the MCMC method. Second, we study the TEOs in these objects and then identify the pulsation phases and mode of the TEOs. The pulsation phases of the TEOs in TIC 266809405, TIC 266894805, and TIC 412881444 are consistent with the dominant $l = 2$, $m = 0$, or ± 2 spherical harmonic. For TIC 11619404, although the TEO phase is close to the $m = +2$ mode, the $m = 0$ mode cannot be excluded because of the low inclination in this system. The TEO phase in TIC 447927324 shows a large deviation ($> 2\sigma$) from the adiabatic expectations, and we suggest that it is expected to be a traveling wave rather than a standing wave.

In addition, an interesting feature of these TEOs is that they occur at relatively low orbital harmonics. A similar situation was also found in the TESS HBSs reported by Kolaczek-Szymański et al. (2021). For comparison, the median and maximum values of n for TEOs in the TESS HBSs are lower than those in the Kepler HBSs reported by Li et al. (2024b). We cautiously suggest that this may be an observational bias. After all, these TESS samples have relatively short continuous observing times, while the value for the Kepler HBSs is more than 1400 days. In our future work, we will aim to discover TESS HBSs with higher harmonic n for TEOs.

ACKNOWLEDGEMENTS

This work is partly supported by the International Cooperation Projects of the National Key R&D Program (No. 2022YFE0127300), the National Natural Science Foundation of China (Nos. 11933008 and 12103084), the Basic Research Project of Yunnan Province (Grant Nos. 202201AT070092 and 202301AT070352), the Science Foundation

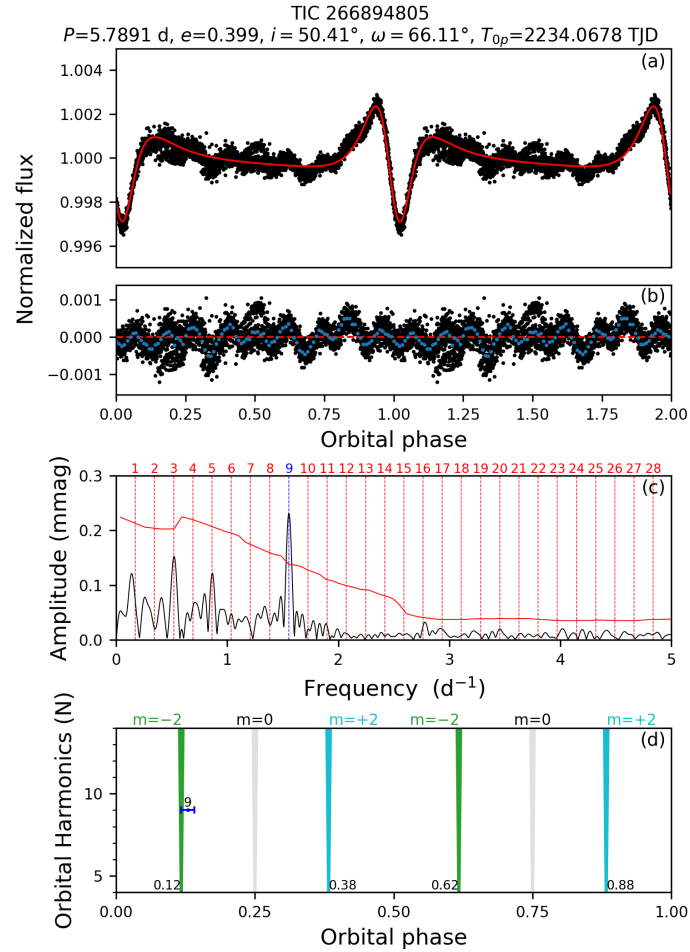


Figure 3. Same as Fig. 1 for TIC 266894805.

of Yunnan Province (No. 202401AS070046), and the Yunnan Revitalization Talent Support Program. The NASA Explorer Program provides funding for the TESS mission. We thank the TESS teams for their support and hard work. We are grateful to the anonymous referee for reviewing this manuscript.

Software: `emcee` (Foreman-Mackey et al. 2013), `lightkurve` (Lightkurve Collaboration et al. 2018), `FNPEAKS` (Z. Koolaczowski, W. Hebisch, G. Kopacki), `PERIOD04` (Lenz & Breger 2005).

REFERENCES

- Borucki, W. J., Koch, D., Basri, G., et al. 2010, *Science*, 327, 977, doi: [10.1126/science.1185402](https://doi.org/10.1126/science.1185402)
- Burkart, J., Quataert, E., Arras, P., & Weinberg, N. N. 2012, *MNRAS*, 421, 983, doi: [10.1111/j.1365-2966.2011.20344.x](https://doi.org/10.1111/j.1365-2966.2011.20344.x)
- Cleveland, W. S. 1979, *Journal of the American statistical association*, 74, 829
- Foreman-Mackey, D., Hogg, D. W., Lang, D., & Goodman, J. 2013, *PASP*, 125, 306, doi: [10.1086/670067](https://doi.org/10.1086/670067)
- Fuller, J. 2017, *MNRAS*, 472, 1538, doi: [10.1093/mnras/stx2135](https://doi.org/10.1093/mnras/stx2135)
- Fuller, J., & Lai, D. 2012, *MNRAS*, 420, 3126, doi: [10.1111/j.1365-2966.2011.20237.x](https://doi.org/10.1111/j.1365-2966.2011.20237.x)
- Guo, Z. 2020, *ApJ*, 896, 161, doi: [10.3847/1538-4357/ab911f](https://doi.org/10.3847/1538-4357/ab911f)
- Guo, Z., Fuller, J., Shporer, A., et al. 2019, *ApJ*, 885, 46, doi: [10.3847/1538-4357/ab41f6](https://doi.org/10.3847/1538-4357/ab41f6)
- Guo, Z., Gies, D. R., & Fuller, J. 2017, *ApJ*, 834, 59, doi: [10.3847/1538-4357/834/1/59](https://doi.org/10.3847/1538-4357/834/1/59)
- Guo, Z., Ogilvie, G. I., Li, G., Townsend, R. H. D., & Sun, M. 2022, *MNRAS*, 517, 437, doi: [10.1093/mnras/stac2611](https://doi.org/10.1093/mnras/stac2611)
- Guo, Z., Shporer, A., Hambleton, K., & Isaacson, H. 2020, *ApJ*, 888, 95, doi: [10.3847/1538-4357/ab58c2](https://doi.org/10.3847/1538-4357/ab58c2)

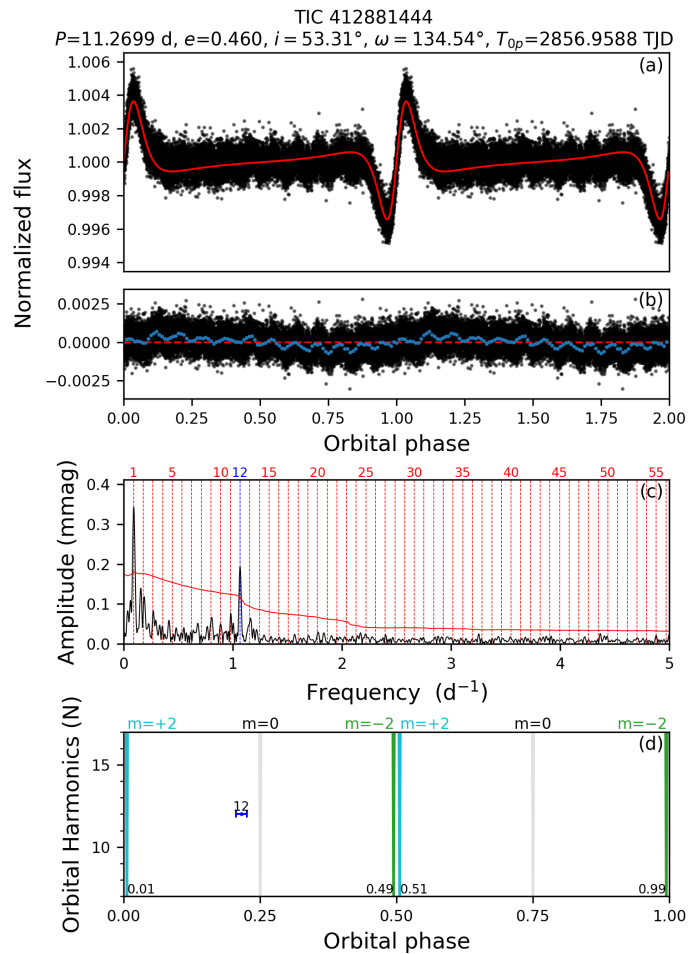


Figure 4. Same as Fig. 1 for TIC 412881444.

Hambleton, K., Kurtz, D. W., Prša, A., et al. 2016, *MNRAS*, 463, 1199, doi: [10.1093/mnras/stw1970](https://doi.org/10.1093/mnras/stw1970)

Hambleton, K. M., Kurtz, D. W., Prša, A., et al. 2013, *MNRAS*, 434, 925, doi: [10.1093/mnras/stt886](https://doi.org/10.1093/mnras/stt886)

Jackiewicz, J. 2021, *Frontiers in Astronomy and Space Sciences*, 7, 102, doi: [10.3389/fspas.2020.595017](https://doi.org/10.3389/fspas.2020.595017)

Jayasinghe, T., Stanek, K. Z., Kochanek, C. S., et al. 2019, *MNRAS*, 489, 4705, doi: [10.1093/mnras/stz2460](https://doi.org/10.1093/mnras/stz2460)

Jayasinghe, T., Kochanek, C. S., Strader, J., et al. 2021, *MNRAS*, 506, 4083, doi: [10.1093/mnras/stab1920](https://doi.org/10.1093/mnras/stab1920)

Kallinger, T., Reegen, P., & Weiss, W. W. 2008, *A&A*, 481, 571, doi: [10.1051/0004-6361:20077559](https://doi.org/10.1051/0004-6361:20077559)

Kołaczek-Szymański, P. A., Lojko, P., Pigulski, A., Różański, T., & Moździerski, D. 2024, *A&A*, 686, A199, doi: [10.1051/0004-6361/202348104](https://doi.org/10.1051/0004-6361/202348104)

Kołaczek-Szymański, P. A., Pigulski, A., Michalska, G., Moździerski, D., & Różański, T. 2021, *A&A*, 647, A12, doi: [10.1051/0004-6361/202039553](https://doi.org/10.1051/0004-6361/202039553)

Kołaczek-Szymański, P. A., Pigulski, A., Wrona, M., Ratajczak, M., & Udalski, A. 2022, *A&A*, 659, A47, doi: [10.1051/0004-6361/202142171](https://doi.org/10.1051/0004-6361/202142171)

Kołaczek-Szymański, P. A., & Różański, T. 2023, *A&A*, 671, A22, doi: [10.1051/0004-6361/202245226](https://doi.org/10.1051/0004-6361/202245226)

Kumar, P., Ao, C. O., & Quataert, E. J. 1995, *ApJ*, 449, 294, doi: [10.1086/176055](https://doi.org/10.1086/176055)

Lenz, P., & Breger, M. 2005, *Communications in Asteroseismology*, 146, 53, doi: [10.1553/cia146s53](https://doi.org/10.1553/cia146s53)

Li, M.-Y., Qian, S.-B., Zhu, L.-Y., et al. 2023, *ApJS*, 266, 28, doi: [10.3847/1538-4365/acca13](https://doi.org/10.3847/1538-4365/acca13)

Li, M.-Y., Qian, S.-B., Zhu, L.-Y., et al. 2024a, *MNRAS*, 530, 586, doi: [10.1093/mnras/stae885](https://doi.org/10.1093/mnras/stae885)

Li, M.-Y., Qian, S.-B., Zhu, L.-Y., et al. 2024b, *ApJ*, 962, 44, doi: [10.3847/1538-4357/ad18c1](https://doi.org/10.3847/1538-4357/ad18c1)

Lightkurve Collaboration, Cardoso, J. V. d. M., Hedges, C., et al. 2018, *Lightkurve: Kepler and TESS time series analysis in Python*, *Astrophysics Source Code Library*, record ascl:1812.013. <http://ascl.net/1812.013>

MacLeod, M., & Loeb, A. 2023, *Nature Astronomy*, doi: [10.1038/s41550-023-02036-3](https://doi.org/10.1038/s41550-023-02036-3)

Montgomery, M. H., & O'Donoghue, D. 1999, *Delta Scuti Star Newsletter*, 13, 28

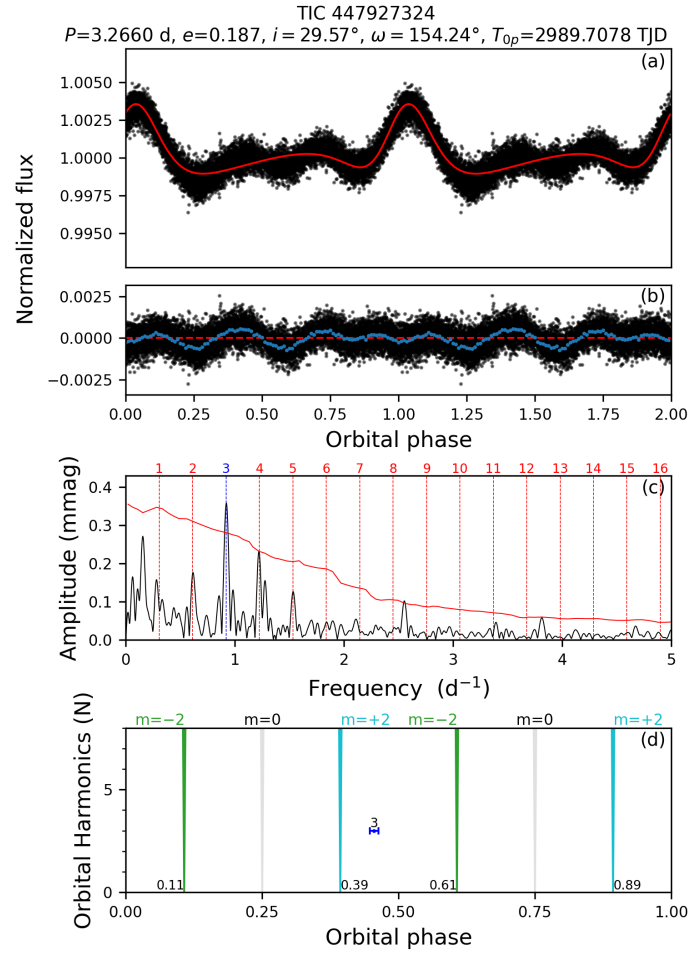


Figure 5. Same as Fig. 1 for TIC 447927324.

O’Leary, R. M., & Burkart, J. 2014, MNRAS, 440, 3036, doi: [10.1093/mnras/stu335](https://doi.org/10.1093/mnras/stu335)

Ricker, G. R., Winn, J. N., Vanderspek, R., et al. 2015, Journal of Astronomical Telescopes, Instruments, and Systems, 1, 014003, doi: [10.1117/1.JATIS.1.1.014003](https://doi.org/10.1117/1.JATIS.1.1.014003)

Thompson, S. E., Everett, M., Mullally, F., et al. 2012, ApJ, 753, 86, doi: [10.1088/0004-637X/753/1/86](https://doi.org/10.1088/0004-637X/753/1/86)

Wang, K., Ren, A., Andersen, M. F., et al. 2023, AJ, 166, 42, doi: [10.3847/1538-3881/acdac9](https://doi.org/10.3847/1538-3881/acdac9)

Welsh, W. F., Orosz, J. A., Aerts, C., et al. 2011, ApJS, 197, 4, doi: [10.1088/0067-0049/197/1/4](https://doi.org/10.1088/0067-0049/197/1/4)

Wrona, M., Kołaczek-Szymański, P. A., Ratajczak, M., & Kozłowski, S. 2022, ApJ, 928, 135, doi: [10.3847/1538-4357/ac56e6](https://doi.org/10.3847/1538-4357/ac56e6)

Zahn, J. P. 1975, A&A, 41, 329